GROUP 7

AIRCRAFT DESIGN FINAL DESIGN REVIEW

March 20, 2013

Sagun Bajracharya
Roger Francis
Tim Tianhang Teng
Guang Wei Yu

Abstract

This document summarizes the work that group 7 has done insofar regarding the design of a radio-controlled plane with respect to the requirements that were put forward by the course (AER406, 2013). This report follows the same format as the presentation where we inform the reader where the current design is, how the group progressed towards that design and how we started. This report also summarizes a number of the important parameters required for a conceptual design like the cargo type & amount,Wing aspect ratio, Optimum Airfoil lift(C_L), Thrust to weight ratio & Takeoff distance. In addition, this report presents the plane's wing and tail design, stability analysis and a mass breakdown. The report finally ends with pictures of the current design.

Contents

List of Figures

List of Tables

1. Design Overview

This aircraft design has essentially evolved to a payload compartment with wings and a tail, in the form of a conventional design. The reason for this design is twofold: Ease of construction and a result of analyzing the scoring function of the course. Since we decided to carry tennis balls for our payload, it is vital that our design of the payload compartment while being large enough to house the balls, also exhibited minimum aerodynamic features required to complete a fast lap of the course, while being light. The current design involves 1.5m span, single tractor and high-wing monoplane. The aircraft is expected to sit within the 1.5m x 1.15m planform limits, maximizing aspect ratio and providing additional length for the fuselage fairing, thus maximizing aerodynamic efficiency. The aircraft is expected to utilize foam/carbon-fiber composite construction for the wing, tail and fuselage internal structure. The fuselage will have detachable high wing, allows easy access to the payload. This payload-focused configuration minimizes the key parameters of system weight through its structural efficiency and access to payloads, while providing sufficient aerodynamic performance and propulsive power density.

2. Required Parameters

In order to create a successful conceptual design, it was determined that a number of parameters needed to finalized. The goal of the first phase of design was to first find these parameters within existing R/C designs and then pass this information through our course requirements and morph the parameters.

- Cargo type & amount
- Wing aspect ratio (AR)
- Optimum Airfoil lift (C_L)
- Thrust to Weight Ratio
- Wing Loading
- Take-off Distance (S_L)

3. Trade Studies

Trade studies were conducted on the three main aspects of the aircraft: the wing, fuselage and tail. Once the trade studies were over, we used the subsequent designs as our baseline for all the research that was done when finding data on existing R/C plane designs.

3.1. Wing Design

There were 3 choices for the types of wing that we could use.

Elliptical
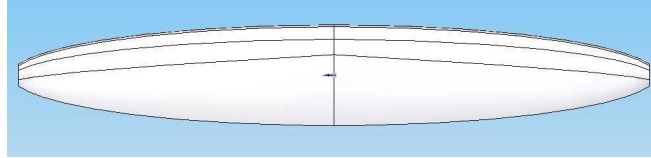
Figure 1: Elliptical Wing

The elliptical wing offers a number of advantages in that it produces the minimum induced drag for a given aspect ratio. Additionally, an elliptical wing also happens to be well suited for heavy payload flights. While the wing is more efficient for L/D, its stall characteristics are quite poor when compared to a rectangular wing. The biggest problem was the manufacturability of an elliptical shaped wing.

Tapered
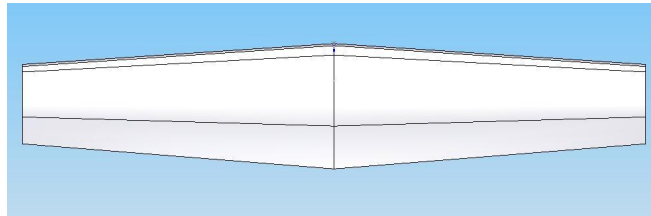
Figure 2: Tapered Wing

The tapered wing was a good option because it provided us with the benefits of an elliptical wing while still being rectangular in shape. The tapered wing also has added advantages of from the standpoint of weight and stiffness. The tapered wing was also a good choice from a weight efficiency point of view since the amount of material as we go away from the root decreases.

Rectangular

The rectangular wing is the best wing for usage from a manufacturability point of view. The rectangular wing has a tendency to stall first at the wing root and provides adequate stall warning, adequate aileron effectiveness, and is usually quite stable. It is also often favored for the design of low cost, low speed R/C planes.
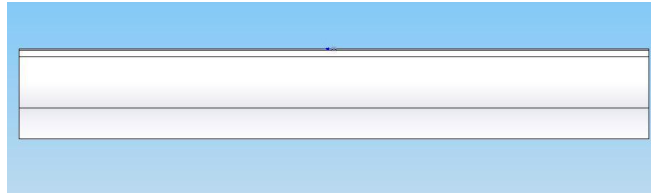
Figure 3: Rectangular Wing

Comparison

Table 1 is the end result of the trade study for the type of wing design. We decided to go with a rectangular wing because it was able to easily beat competing designs based on factors such as construction and flight performance.

Categories	Weighting	**Rectangular**	Elliptical	Tapered
Construction	40%	**5**	2	3
Flight Performance	30%	**3**	3.5	3
Theoretical Analysis	30%	**3**	2	2
Total	100%	**3.8**	2.45	2.7

Table 1: Wing Type Score Table

3.2. Wing Configuration

The second aspect that was studied was the different type of wing designs that we could have.
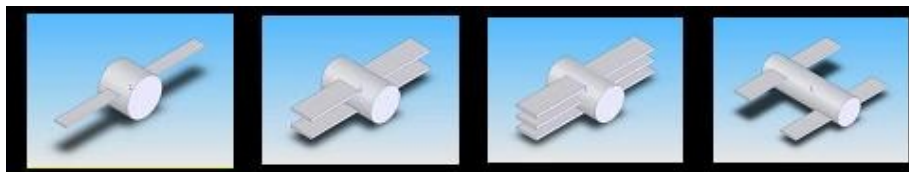
Figure 4: Wing Configuration Options

Typically, the simplicity and performance per weight of the monoplane would make it the frontrunner. Despite this, the span and aspect ratio values we were aiming for made multi-wing aircraft an attractive option. The final result for the wing design is depicted in table 2.

3.3. Fuselage Design

Fuselage studies focused on three different models.

Categories	Weighting	**Monoplane**	Biplane	N-plane	Tandem
Construction	40%	**4**	3.5	1	3.5
Flight Performance	30%	**3**	3.5	3	3
Theoretical Analysis	30%	**3**	3	3	3
Total	100%	**3.4**	3.35	1.1	3.20

Table 2: Wing Configuration Score Table
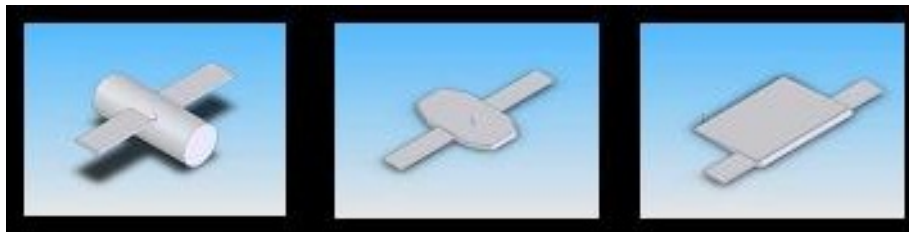
Figure 5: Fuselage Configuration Options

The factors that affected the choice of design was the wing loading characteristics along with the capability of loading flexibility for the different types of balls. While the lifting fuselage could potentially reduce wing loading, there was the potential problem of executing a low-weight construction along with the excessive airfoil thickness to accommodate a variety of potential loads. Additionally, while the flying provided good drag efficiency, a conventional design was found to be often favored within the model building community due to ease of construction and general experience within the R/C community about building conventional aircraft. The results of the trade studies are displayed in table 3.

Categories	Weighting	**Conventional**	Blended	Flying Wing
Construction	30%	**4**	2	3
Weight	20%	**2**	2	4
Flight Performance	20%	**3**	2	3
Theoretical Analysis	30%	**4**	2	2
Total	100%	**3.4**	2	2.9

Table 3: Fuselage Type Score Table

3.4. Tail Design

Finally, Tail design focused on 3 different designs as depicted below.

There were a number of factors that affected the grading in the table below. Namely: While the H-Tail increases effectiveness of the horizontal control surfaces through the winglets, it also adds increased weight to the design since we require a number of vertical surfaces with their
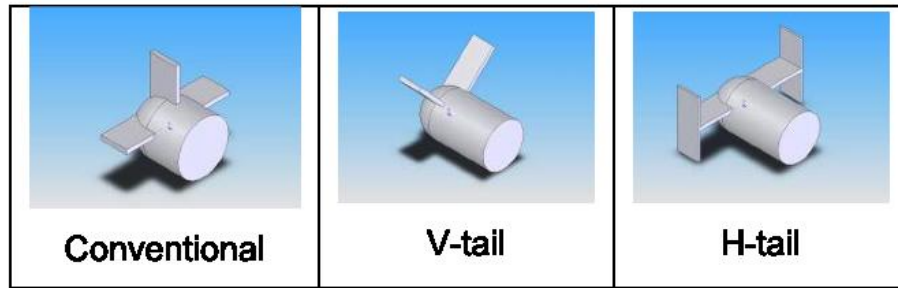
Figure 6: Empennage Configuration Options

control servos, which may not be considerable. While the V-Tail provided a number of benefits, the team felt that we could get the same performance characteristics from a simpler design given the speed we were traveling at. Additionally, no weight was expected to be saved by using a more complicated tail design.

The conventional design is well known for its low risk and ease of control and manufacturability. A conventional design is also widely used in the R/C community because it is the most efficient tail design for the speed R/C planes are expected to fly it. Table 4 shows the final results of the trade studies for tail design.

Categories	Weighting	**Conventional**	T-tail	V-tail
Construction	40%	**4**	2	3
Flight Performance	20%	**3**	3.5	3.5
Theoretical Analysis	30%	**3**	2	2
Total	100%	**3.25**	2.45	2.7

Table 4: Empennage Type Score Table

3.5. Overall Selection

Given the choices of the previous trade studies, the design that turned out to be best option was a tractor R/C plane with a conventional fuselage & tail and a mono wing.

This design choice was based on factors of construction ability, ability to provide accurate analysis, lowest structural weight and largest potential cargo space. Another factor that was also included in the construction factor- was the general amount of problems people had in building the planes.

3.6. Parameters from Reference Designs

Once the design for the plane was decided, research was conducted on existing R/C planes. Resulting reference parameters are shown here.

- Max take-off weight 1.5kg
- Aspect Ratio ≈ 5
- $C_{L_{max}} \approx 1.5$
- Stall Velocity $\approx 7 \sim 8$ m/s

4. Flight Score Optimization

In order to optimize the flight score:

$$FlightScore = CargoUnits \times f \times PF \times TB \times CB \tag{1}$$

the equation was analyzed on a component by component basis. From the trade studies, our group determined that we would use a conventional design and thus our configuration bonus CB = 1.

Due to this loss in potential points, our group determined we would like to get the takeoff bonus (TB) and thus we began our analysis with the assumption that TB = 1.2.

Using the above knowledge, the speed of the aircraft and the cargo units had to be optimized. This was accomplished in a 2 stage optimization. The first stage consisted of optimizing cargo units and PF, while the second step consisted of factoring in the benefits associated with increasing speed, by forgoing cargo.

4.1. Cargo Selection

In order to assess the optimal cargo distribution a plot of the various flight scores vs. total weight of the aircraft were plotted.

Figure 7 shows the various point distributions for ping pong/golf ball configurations and a 10 tennis ball cargo configuration. The 600g, 700g, 800g, 900g, and 1kg planes refer to empty weights of the plane and the Flight score associated with loading such a plane with a permutation of golf balls and ping pong balls. The tennis ball configuration refers to a plane that is fully loaded with 10 tennis balls. Based on group discussions and previous year's designs, an empty weight of 900g was decided as a reasonable estimate for the empty weight of our aircraft. For a tennis ball configuration that would amount to a total weight of $900g + 570g = 1.47kg$ where 570g is the weight of 10 tennis balls. Looking at Figure 7 it is evident that for a ping pong/golf
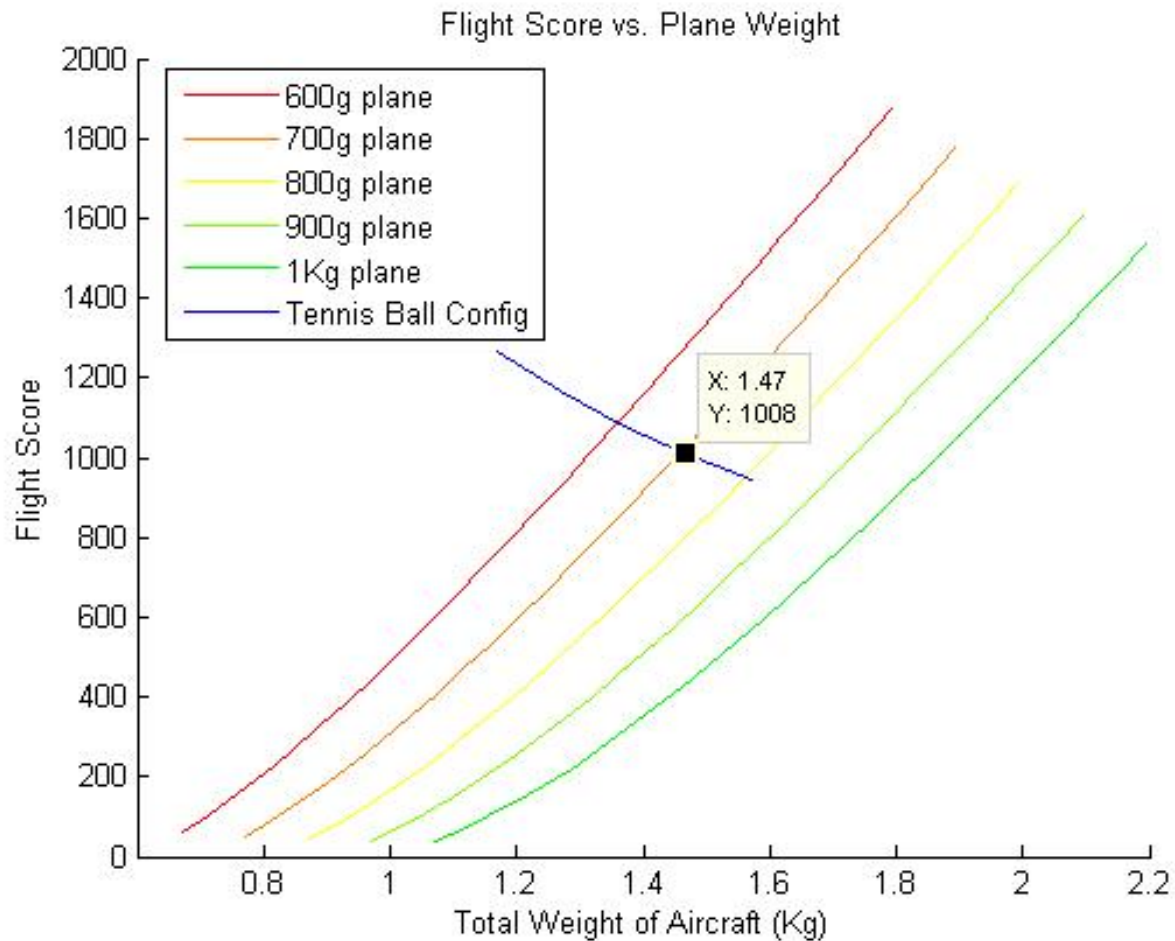
Figure 7: Flight Score Analysis

ball configuration to provide the same flight score as the tennis ball configuration, the empty weight would have to be merely $700g$. Thus, our group decided our aircraft would carry 10 tennis balls as our cargo.

4.2. Propeller Selection

Once the cargo was selected, a proper propeller had to be selected such that the aircraft could take off within $25ft$, to ensure the takeoff bonus, and to optimize the flight score with respect to speed. In order to do this, a few estimates of flight parameters were made.

- $C_{d0} = 0.040$
- $C_l = 0.6$
- $e \approx 0.8$
- $AR = 5$

- $S = 0.3m^2$

- $b = 1m$

Using the above information and the provided equipment:

- Axi -2217-16 Brushless motor

- 1200-1300 15C mAhr battery

- Castel-Creations Thunderbird 18 speed controller

Mottocalc was used to generate a list of suggested propellers and power available for various flight speeds. This information was used in conjunction with the power required formula:

$$P_r = T_r v = \left(qSC_{d0} + \frac{W^2}{qS\pi eAR} \right) v \tag{2}$$

to generate plots of power required vs. power available. Using this information we can determine the optimum propeller configuration. We first analyzed the maximum velocity of our empty plane.

Looking at Figure 8 it is evident that the maximum velocity of the empty aircraft is roughly $16.5m/s$ using a $9'' \times 6''$ propeller. In order to verify that this propeller is sufficient for our take off needs, we then assessed the takeoff performance of this propeller using the following approximation for ground roll:

$$S_g \approx \frac{1.21W}{9.81 \times C_{l_{max}} \times \left[\frac{T}{W} - \frac{D}{W} - \mu \left(1 - \frac{L}{W} \right) \right]_{0.7V_{lo}}} \tag{3}$$

Where V_{lo} is the lift off velocity and is approximated as:

$$V_{lo} = 1.1 \times \sqrt{\frac{2W}{\rho SC_{l_{max}}}} \tag{4}$$

The coefficient of friction for the plywood runway was taken to be $\mu \approx 0.1$ and the maximum lift coefficient was estimated to be $C_{l_{max}} \approx 1.5$. This led us to the estimation that $S_g \approx 15ft$ which is sufficient for the takeoff bonus.

4.3. Flight Parameter Selection

The flight parameters were iteratively updated, from our initial guess above, in order to accommodate a $1.47kg$ plane. This led us to the following design parameters:

- $C_{d0} = 0.040$

- $C_l = 0.6$

- $e \approx 0.8$

- $AR = 5.35$

- $S = 0.42m^2$

- $b = 1.5m$
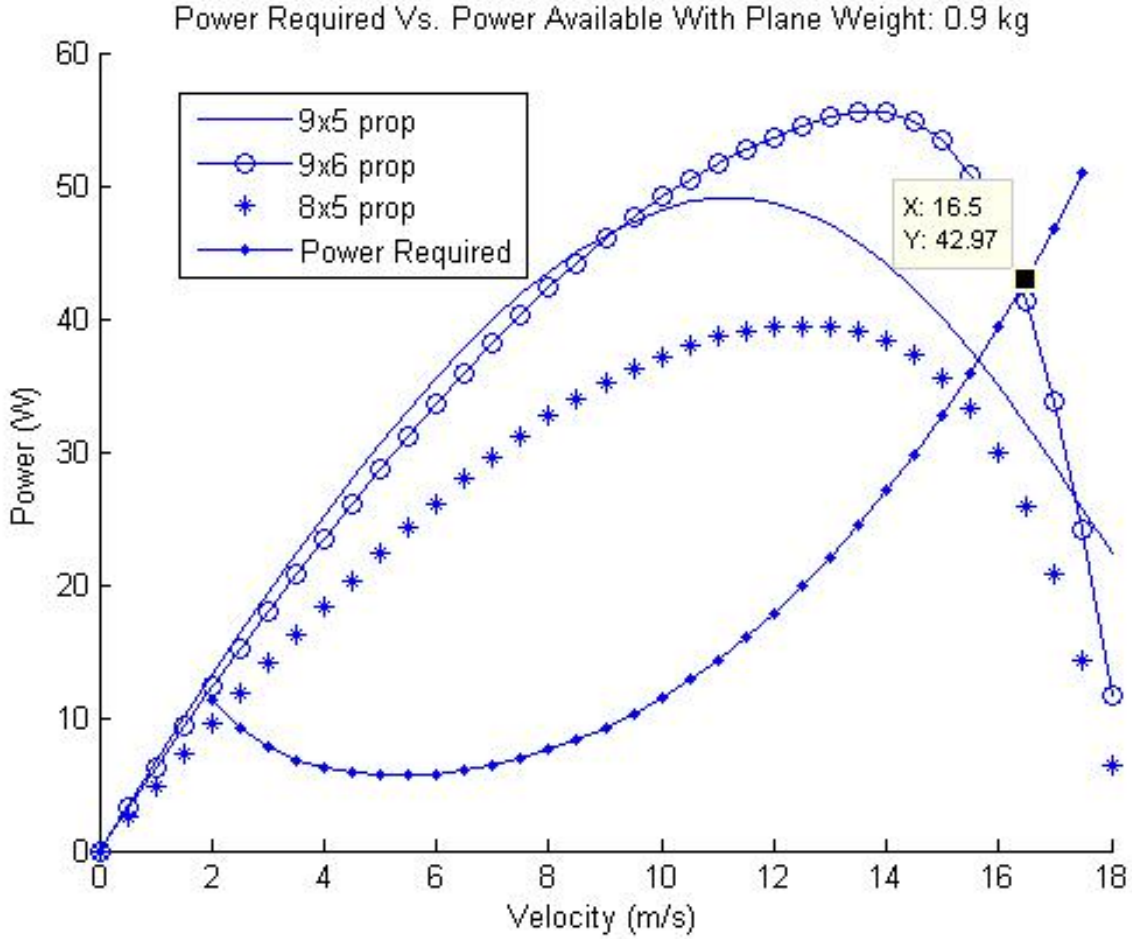
Figure 8: Power Analysis for Plane Weight 0.9kg

Using the above design parameters we would have a takeoff distance of $24ft$. and a maximum velocity defined by the intersection of the power available vs. power required curves:

Looking at Figure 9, it can be seen that the maximum velocity of the aircraft has dropped from $16.5m/s$. For comparison we decided to analyze the penalty associated with decreasing our speed by $0.5m/s$. This was done by approximating the overall flight distance to be roughly $200m$.

Looking at figure 10, we approximated the turn distance at each of the markers to be roughly 30 m while the distance between markers is 70 m. Using this approximation, the nominal velocity to fly at is $\frac{200m}{20s} = 10m/s$. Re-arranging the flight time penalty function gives Eq. 5

$$f = e^{1.5\left(1-\frac{t/200}{t_{nominal}/200}\right)}$$
$$= e^{1.5\left(1-\frac{v_{nominal}}{v}\right)} \tag{5}$$

As can be seen in figure 11, the penalty associated with reducing the speed by 0.5 m/s is only

14
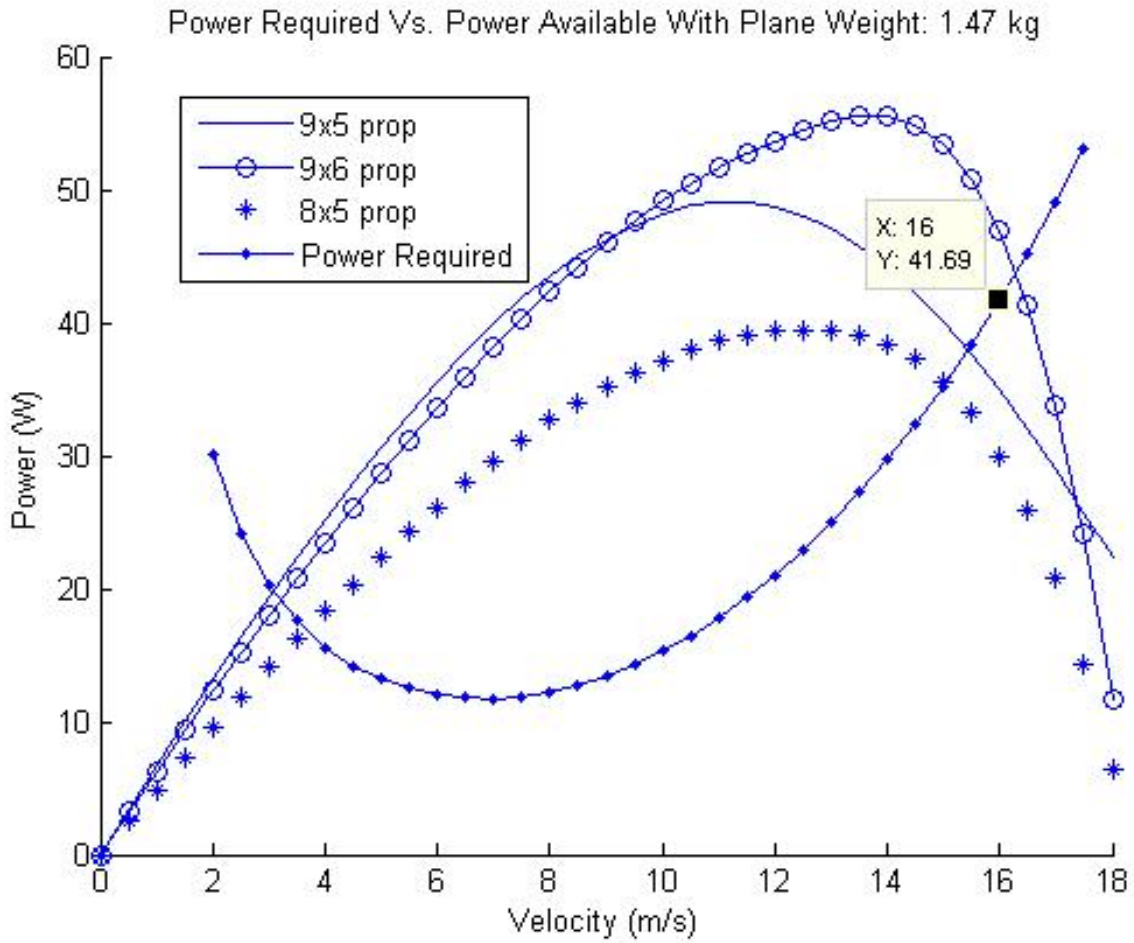
Figure 9: Power Analysis for Plane Weight 1.47kg
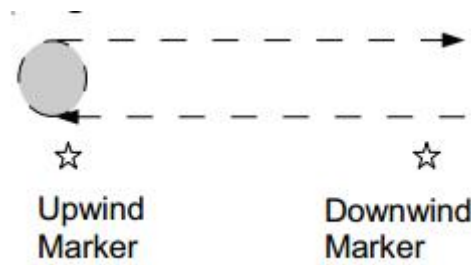
Figure 10: Approximate Flight Path

0.05 thus we decided the current propeller selection and flight parameters were sufficient for the initial design.
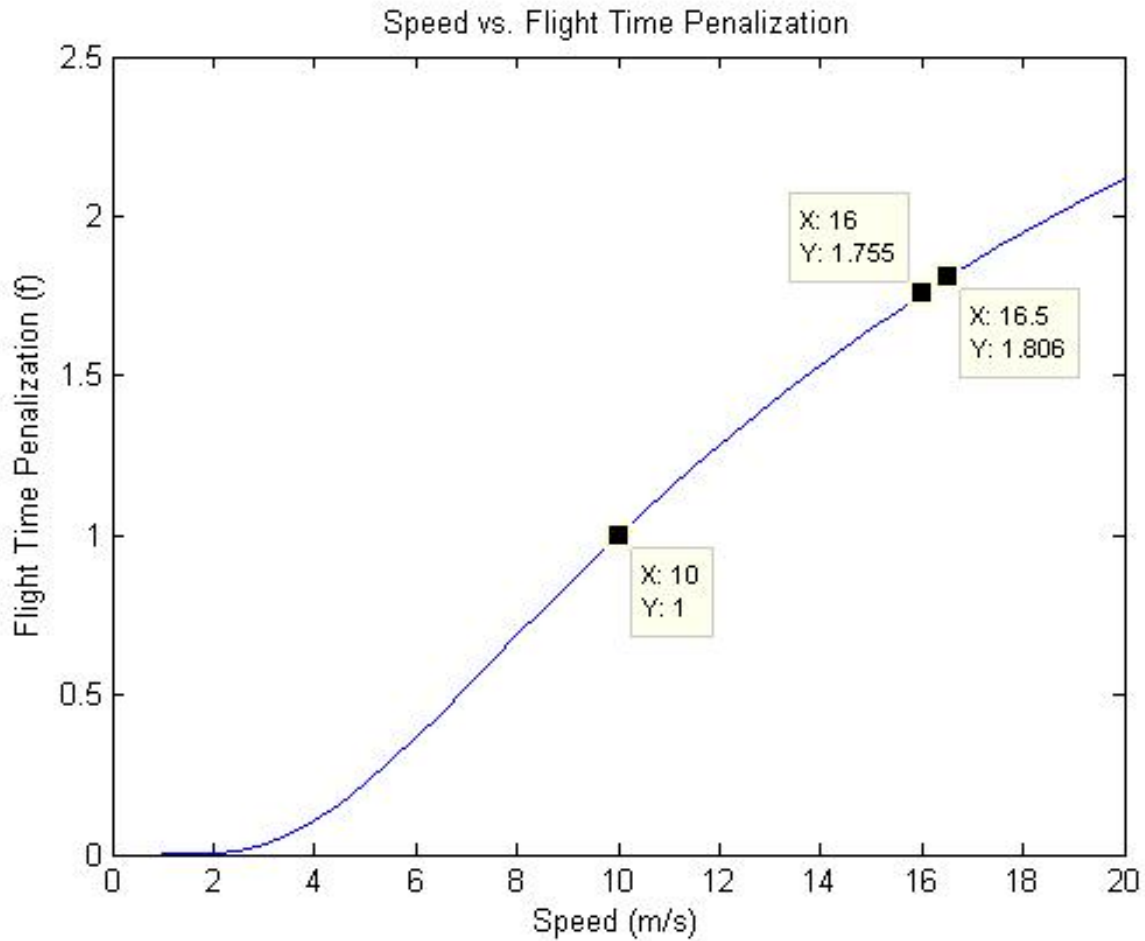
Figure 11: Time Penalization Factor vs. Speed

5. Wing Design

One of the most important components of an aircraft design is the wings. The wing is the main contributor of lift, drag, and stability. The design of a wing is an iterative process, however the preliminary design can be divided into multiple aspects: the wing shape, wing position, configuration, taper, sweep, airfoil selection, as well as the physical dimension.

5.1. Wing Position

One of the initial considerations to be made when designing the wing is the position of the wing. Historically, aircraft wings have been installed on various locations on the wing to accomplish different objectives. Below are a few common wing positions.

In the proposed design, a high wing structure configuration is used. The high wing configuration allows both side of the wing to be joined into a single piece. This configuration raises the wing higher above the ground, reducing the ground effect during takeoff and landing. The configuration
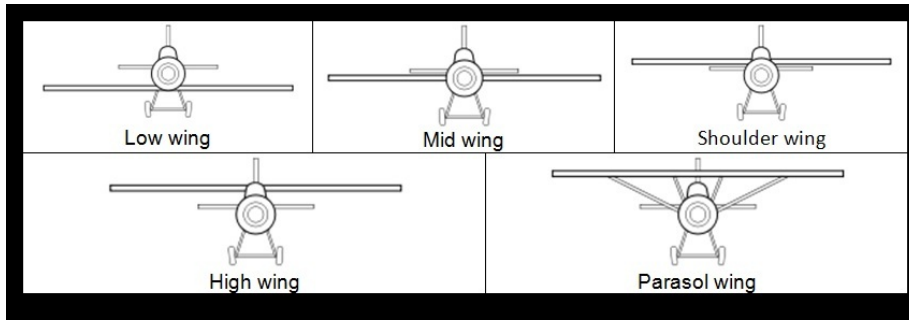
Figure 12: Possible Wing Position

also adds stability to the aircraft, as more of the weight is now hanging underneath the wing. Not only does a high wing provide more desirable aerodynamic performances, it also aids in the structural and design aspects. The continuous nature of a high wing avoids the use a joints that links the wing to the fuselage. This reduces the discontinuity in the shear flow in the wing, and allows the wing to sustain more bending moment before breaking.

Lastly, a high wing is easier to manufacture. Manufacturability is often a major concern in the design of an aircraft. A high wing allows a single piece of the wing to be attached to the top of the fuselage, enabling easier attachment of the wing, and making repositioning of the wing a possibility. With a high wing, the wing itself can even become a door to the cargo area, where the entire wing could be lifted off during cargo loading, and reattached easily prior to flight.

5.2. Sweep
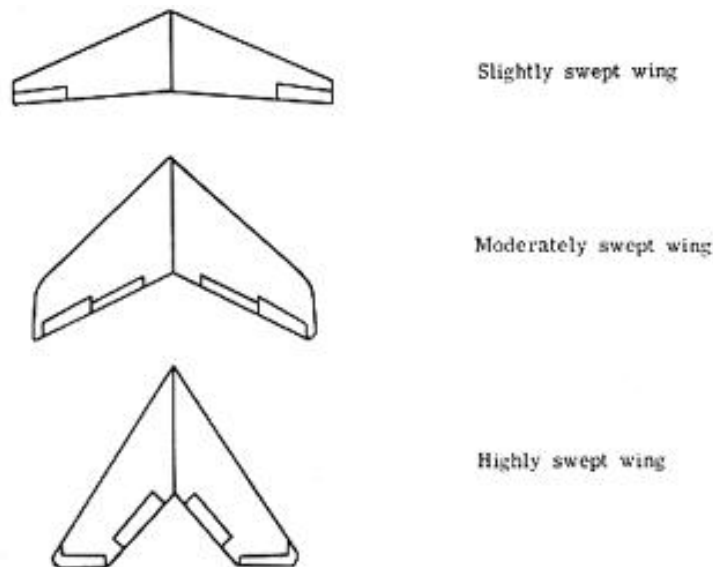
Figure 13: Wing Sweep Options

Wing sweep is another common feature. In many commercial designs, wings are swept back to create a seemingly larger chord. The sweep is beneficial to the yaw stability of the aircraft, due to a higher lift induced on the wing which the aircraft is yawing, creating a returning moment to cause the aircraft to turn back to proper direction. In addition, a swept back wing aids at reducing the drag on the wing, as the wetted area becomes smaller. Sweep wing are also beneficial in high speed aircrafts, as it allows the aircraft to reach speed closer to Mach 1 without the wing going supersonic. Despite these benefits, the main concern with designing a swept wing is the manufacture difficulty. A swept back wing and its benefits would not be dominate in the flight condition of the proposed aircraft, and thus sweep was not implemented in the proposed aircraft.

5.3. Taper

Wing designers often add taper to the wing to make the wing more efficient. From aerodynamics, a wing is most efficient in an elliptical configuration. Adding taper to a wing cause it to behave more elliptical. Tapering a wing increases the aspect ratio, which contributes to many performance benefits such as reduction in lift induced drag, more range, and better climb rate. Adding taper to wings can also be structurally efficient. A wing experiences larger moment closer towards the root of the wing. A tapered wing has an increased chord at the root of the wing, and reduces the chord towards the tip of the wing. This allows the structure of the wing to be focuses on the area of greater stress, and thus making the wing more structurally efficient.
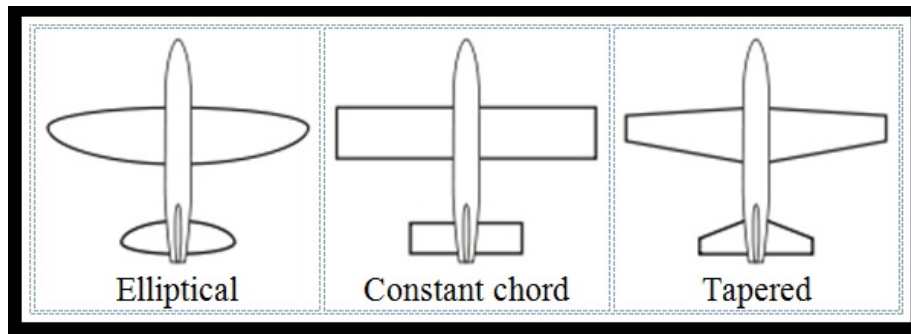
Figure 14: Taper Options

However, tapered wing suffers from a reduced roll rate. As analyzed in the previous sections, one of the key design targets is to minimize the time for the aircraft to loop around the field. This implies a faster roll rate and thus tighter turning radius is desired. By increasing the taper, a wing is also required to have a longer span, which often adds to the weight of the wing. With these considerations, along with the manufacturability difficulty of manufacturing a tapered wing, it is decided that the benefits associated with a tapered wing is not sufficient, and thus tapering is not incorporated in the proposed design.

5.4. Wing Size

Next, the size of the wing is determined. Immediately obvious is the effect of wing size on the aerodynamic performances of the wing. It is know (Eq. 6) that both the lift and drag of the wing is directly proportional to the area (S) of the wing.

$$L = qSC_L \tag{6}$$
$$D = qS \left(C_{d0} + \left(\frac{1}{\pi e AR} \right) C_L^2 \right)$$

From previous score analysis, the aircraft should carry more load, at the same time accomplish the flight path in minimal amount of time. To compromise between the two competing factors, an analysis is done on the effect of lift and drag on the desired performance. The lift of the aircraft is mainly associated with the amount of cargo unit it can carry. Higher lift from the wings means the aircraft can carry more load and while sustain flight. Also, increasing the lift of the wing is beneficial to the takeoff distance and climb rate. Increasing the lift implies a reduction in the power required for the aircraft to maintain leveled flight. This means there are more excess power for the aircraft to climb and maneuver. Increasing the lift also allows the aircraft to bank at a steeper angle, thus contributing to a smaller turning radius. The increase in drag resulted from increasing in S is also dominant. Higher drag increases the power required to fly, and reduces the speed the aircraft can fly. These effects countered the benefits gained by increasing lift, and thus a balance has to be draw to maximize the flight score. From previously conducted iteration on the flight score, a final wing area is selected to be $0.42m^2$. At this area, the lift at drag exists at a balance such that in a typical flying condition, the score would be maximized.

5.5. Airfoil Selection

Lastly, the airfoil of the main wing is selected. Much consideration went into the selection of the airfoil. Firstly, the airfoil should have a high C_L to increase the lift without increasing the S too much. Next, the airfoil should have a high $C_{L_{max}}$ in order to reduce the takeoff distance. The airfoil should also have a high stall angle of attack, to reduce the risk of stalling during climb. Lastly, for manufacturing purposes, the lower surface of the wing should be as flat as possible to make attaching the wing simpler.

The airfoils that were considered are listed in appendix C.

From the comparison, a symmetrical airfoil such as NACA 0012 has significantly lower max CL and lower stall angle. Further investigation into cambered airfoils yields the above selections of CLARK Y and CLARK YM-15, as well as the GOE 526 reveals that only the GOE 526 and CLARK YM-15 have high enough max CL for the proposed design. In addition, the GOE 526

has a significantly higher 'lower surface flatness', making manufacturing easier.

The final selection is the **GOE 526 Airfoil**. The specification as well as the drag polar of the airfoil is shown in Fig 15.
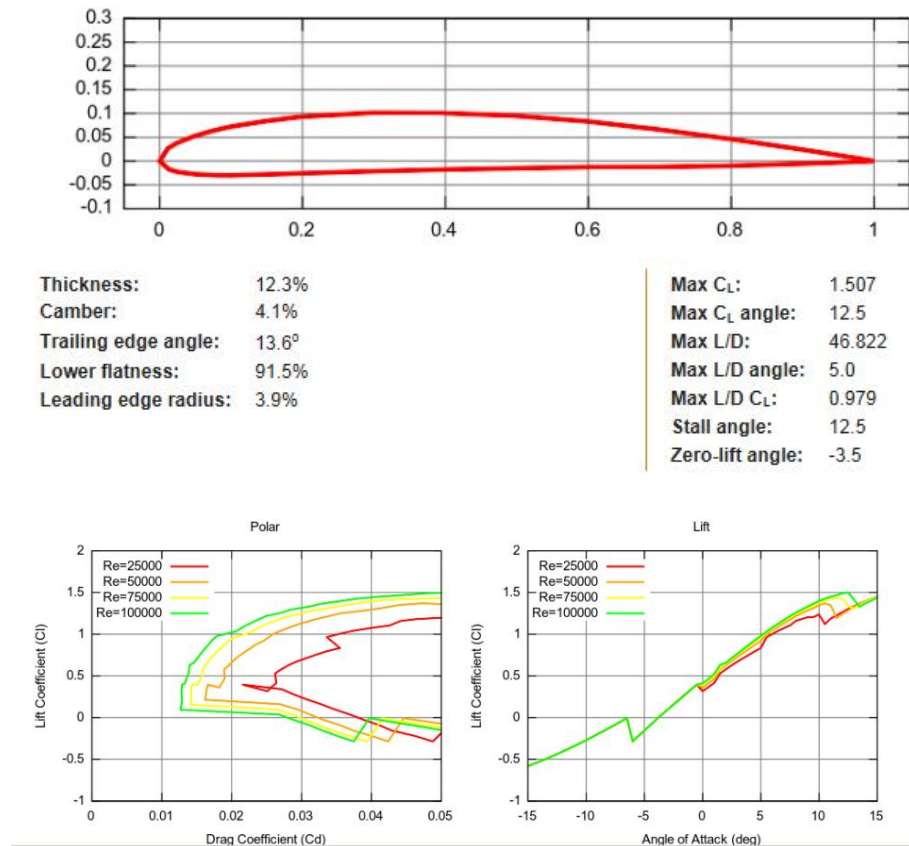
Figure 15: Airfoil Data

This airfoil is a cambered airfoil with a lower surface flatness of 91.5%. The airfoil has a maximum C_L of 1.5, and a stall angle of 12.5 degrees. These specifications of the airfoil was inputted into the MATLAB code discussed in the previous section, and the specifications satisfies the criteria for the design. It is also decided that to increase the C_L of the wing to maximize lift capabilities, the airfoil is going to be attached to the fuselage with a 5 degrees angle of attack. The 5 degrees angle also matches the max L/D angle of the airfoil, thus making the design more efficient.

5.6. Wing Design Specification

With the above discussion on the features of the wing, a finalized wing design is generated. Shown below is a drawing of the proposed wing.
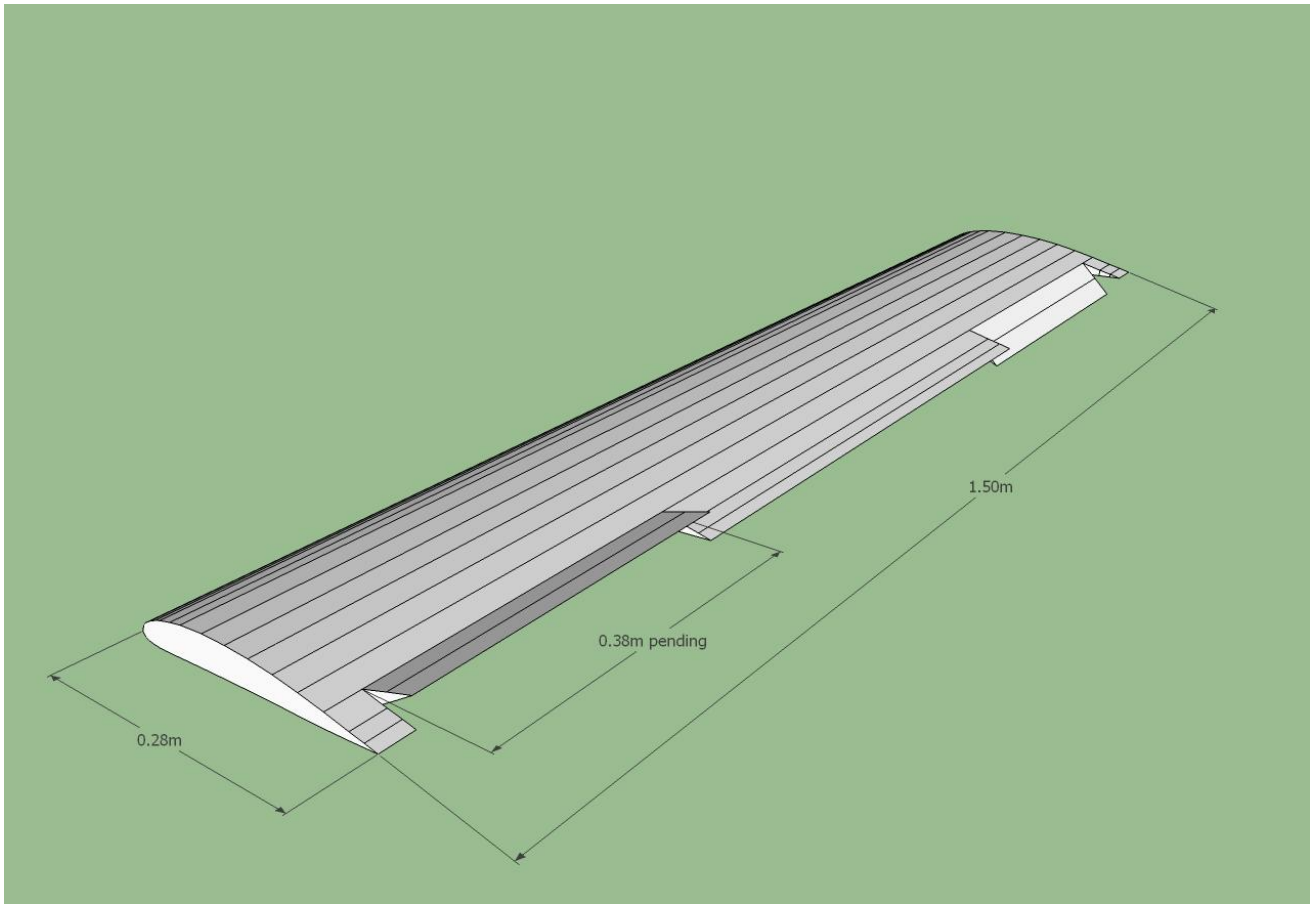
Figure 16: Engineering Drawing of our Wing Design

The detailed specifications of the wing is listed in table 5:

5.7. Wing Performance

With the above design, a preliminary performance estimate for the aircraft is done. A common parameter for wing design is the L/D ratio. This is estimated to be around 15.8 during cruise flight. This value seems reasonable at this point of design, as a Boeing 747 have a L/D or 17. Next the wing loading is examined. The wing loading is defined in Eq 7

$$WingLoading = \frac{W}{S} \tag{7}$$

This parameter is a indication of the maneuverability of the aircraft, where a lower wing loading allows the aircraft to perform better. The wing loading for the proposed wing is estimated to be $3.1 kg/m^2$.

Lastly, the load factor of the wing is examined. The cruise lift / weight is estimated to be 1.82, which denotes that the aircraft is able to generate much higher lift than it requires in cruise. These excess lift can contribute to turning capability, thus leads to a higher time score. The

Specification	Value
S	$0.42m^2$
AR	5.3
Chord	$0.28m$
Span	$1.5m$
α_0	$5°$
C_{L0}	0.64
L_{Cruise}	$23.7N$
D_{Cruise}	$1.5N$

Table 5: Wing Design Specification Table

turning performance of the aircraft is governed by Eq 8

$$R = \frac{V^2}{g\sqrt{n^2 - 1}}, \qquad n = \frac{L}{W} = 1.82 \tag{8}$$

From this calculation, the turning radius of the aircraft is estimated to be 7.6m, where the turning radius of an aircraft with n = 1.47 would be 15m. By increasing the lift to weight by 0.4, the turning radius decreased by half.

6. Empennage Design

This section outlines design of horizontal and vertical stabilizer with consideration to static longitudinal and lateral stability. The Stability performance and design is outlined in further detail in section 7. Important consideration in empennage design additionally include control surface parameters are determined using literature and control derivative through simulation with XFLR5. Mainly the roll authority was considered. With varying airfoil by introducing opposite flaps in Xfoil, the control derivative $c_{l_{\delta_a}}$ is estimated, which is then used to calculate the demensionalized control derivative $C_{l_{\delta_a}}$ for design geometries.

Final design is outlined in section 6.1 and section 6.2.

6.1. Horizontal Stabilizer

H-stab Desgin

- H-stab Span $0.58m$

- H-stab CG to Aircraft CG $l_t \approx 0.75m$

- H-stab Chord $c_t = 0.14m$

- Horizontal Tail Volume $V_H = 0.52$

- H-stab Airfoil NACA0012

Aileron Desgin

- Fuselage to Aileron distance $b1 = 0.3m$ along y-axis

- Fuselage to Aileron distance $b2 = 0.7m$ along y-axis

- Aileron Depth 25% chord $0.07m$

- Aileron Surface Area $0.056m^2(13.33\%$ wing area)

6.2. Vertical Stabilizer

V-stab Desgin

- V-stab Root Chord $0.14m$

- V-stab Sweep $16.7°$

- V-stab Height $0.15m$

- V-stab Area $0.0165m^2$

Rudder Desgin

- Rudder Depth $0.58m$

- Fuselage to Rudder distance $b1 = 0.05m$ along z-axis

- Fuselage to Rudder distance $b2 = 0.15m$ along z-axis (maximum height)

6.3. Theoretical Performance

An important aspect of the tail design is to examine the aircraft's overall performance with the addition of the tail. We have modeled the aircraft as a wing and tail configuration at the proper geometry setting and examined the combined lift performance.

The analysis indicates that sufficiently linear coefficient of lift versus angle of attack of the wing is achieved for probable range of flight condition. This is shown in figure 17 and the star at $C_{L,\alpha=4°} = 0.67$ indicates condition at take-off and appropriate C_L value (see Section 4.3) is generated with the initial angle of attack on the wing.

The combined lift is optimized for various tail offset angle and the best angle was found to be $\alpha_t = \alpha - 5°$ from angle of attack of wing (α).
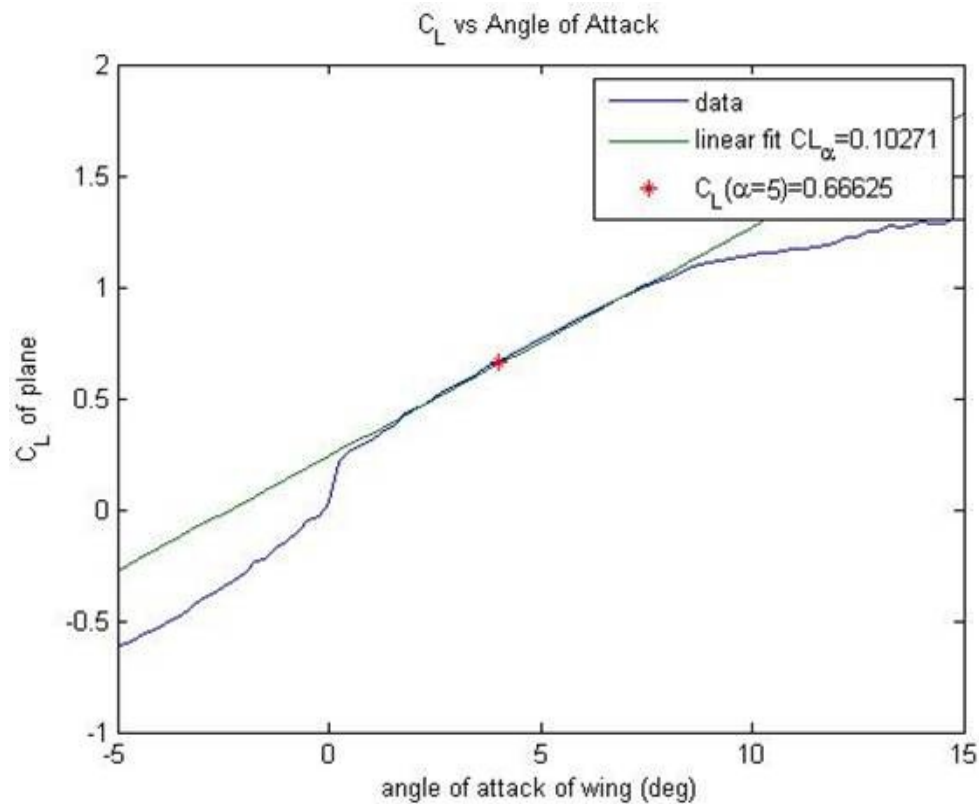
Figure 17: Combined C_L performance

7. Stability

In consideration to stability of our model aircraft, we have considered static as well as dynamic stability. Static stability is considered from early phase of our design beginning with simplified back of the envelope calculations and iterations with detailed mass and force distribution using MATLAB. Furthermore, XFLR5 is used to aid stability analysis by providing stability derivatives for assumed flight conditions and solving eigenvalue problem pertaining to the dynamic stability mode analysis. We have determined through iterative design approach between mass CG and stability as well as performance measures for some suitable values of horizontal and vertical tail volume found in literature. This parameter ensures controllability given the wing as well as some sense of stability, and design is verified through XFLR static and dynamic stability analysis. The iterative method include balancing center of gravity (CG) of the aircraft as well as stability parameters such as neutral point and aerodynamic center of the wing(see section 7) and monitoring the stability measures.We provide an analysis of the static and dynamic stability of final design here.

24

7.1. Static Stability

For static stability, main design concern revolve around longitudinal static stabilities for conventional design. Two criteria governing longitudinal stability consideration are summarized in Eq 8a and 8b.

$$\frac{\partial C_M}{\partial \alpha} < 0 \tag{8a}$$

$$C_{M,\alpha=0} > 0 \tag{8b}$$
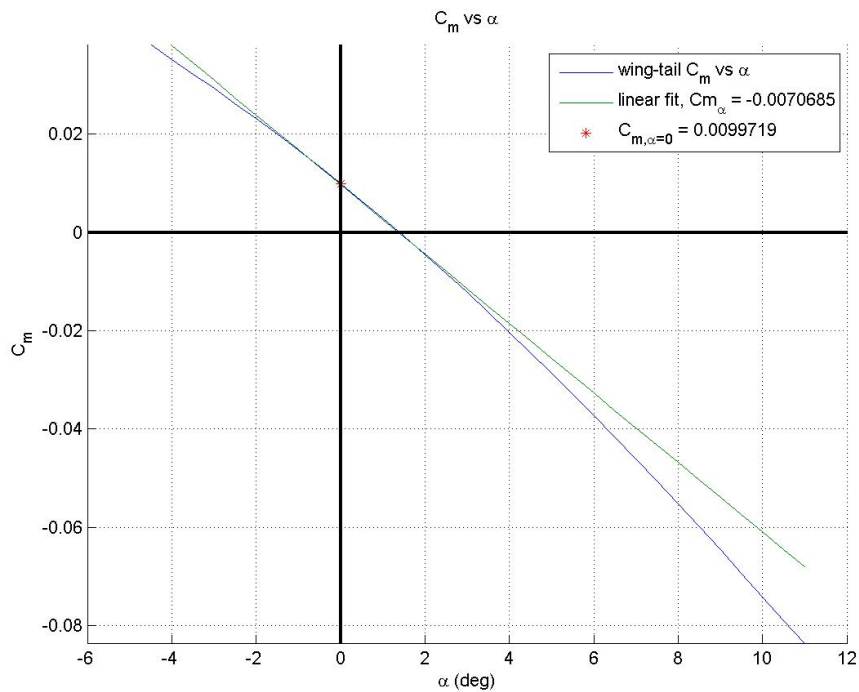
Figure 18: Combined C_M performance

Combined Moment Coefficient   Similar to the combined lift, we have computed the combined moment from iterated design geometries considering aerodynamic center and neutral point, in combination with CG of the aircraft. The combined moment plot versus angle of attack of wing in figure18 indicates a nice negative slope for stability until a relatively large angle of attack. We have also shown a static margin with respect to mean aerodynamic chord (MAC) of 10.7%.

The star point at zero angle of attack shows the aircraft's initial positive moment, and the presence of zero C_M shows the aircraft's ability to trim.

We can thus conclude that our preliminary design is theoretically longitudinally stable.

Longitudinal Static Stability Parameters

A more detailed graphical visualization of our stability parameters with respect to loading can be seen in Figure 22 of Appendix A. The detailed longitudinal static stability parameters are listed as follows.

- Neutral Point from Tip is $496.91mm$.

- Aerodynamic Center from Tip is $420mm$.

- Aircraft CG from Tip is $472.03mm$.

- Stability Margin is $9\%MAC$.

- $\frac{\partial C_M}{\partial \alpha} \approx -0.007$.

7.2. Dynamic Stability

Dynamic stability analysis involved mainly looking at stability derivatives to estimate dynamic modes and time simulation of aircraft to perturbation. The result shows that all of our longitudinal dynamic modes are stable with good damping where handling quality is concerned. For lateral stability, we have unstable spiral mode characteristic of conventional design. However, the time to double is found to be 13.8 seconds. Even though analysis does not consider the dihedral effect of the high wing configuration, the extra margin from 5 seconds required from pilot is sufficient for controllability although there presents instability in this mode. The detailed dynamic stability parameters are listed in table 6.

Modes	Eigen Values	Period	Damping
Short Period	$-13.8316 \pm 6.3223i$	0.413s	0.91
Phugoid	$-0.0438 \pm 0.3333i$	18.87s	0.13
Spiral	0.0503	N/A	N/A
Roll Damping	-59.7392	N/A	N/A
Dutch Roll	$-1.0861 \pm 6.3796i$	0.97s	0.168

Table 6: Dynamic Stability Mode Results Table

The stability is confirmed by looking at the root locus plot for longitudinal and lateral dynamic modes shown in figure 19 and figure 20. A time simulation corresponding to the lateral instability is shown in figure 21. This simulation shows the spiral mode under unit perturbation growing. The time to double is roughly 13.8 seconds which gives enough controllability with a margin for neglecting dihedral effect of high wing.
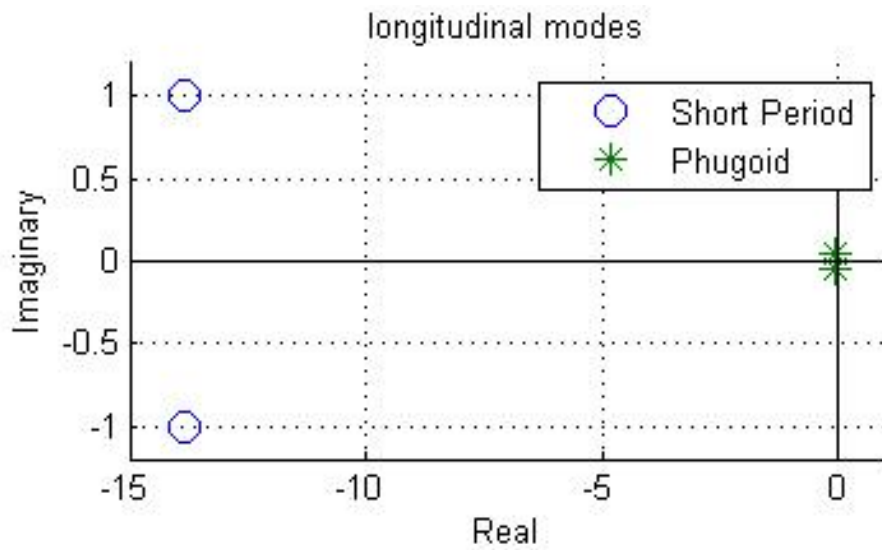
Figure 19: Longitudinal Dynamic Modes Root Locus Plot
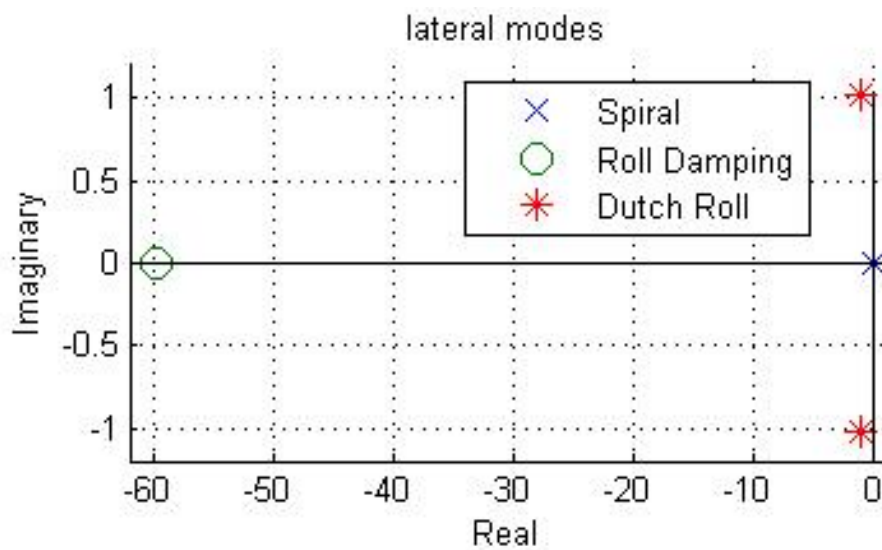
Figure 20: Lateral Dynamic Modes Root Locus Plot
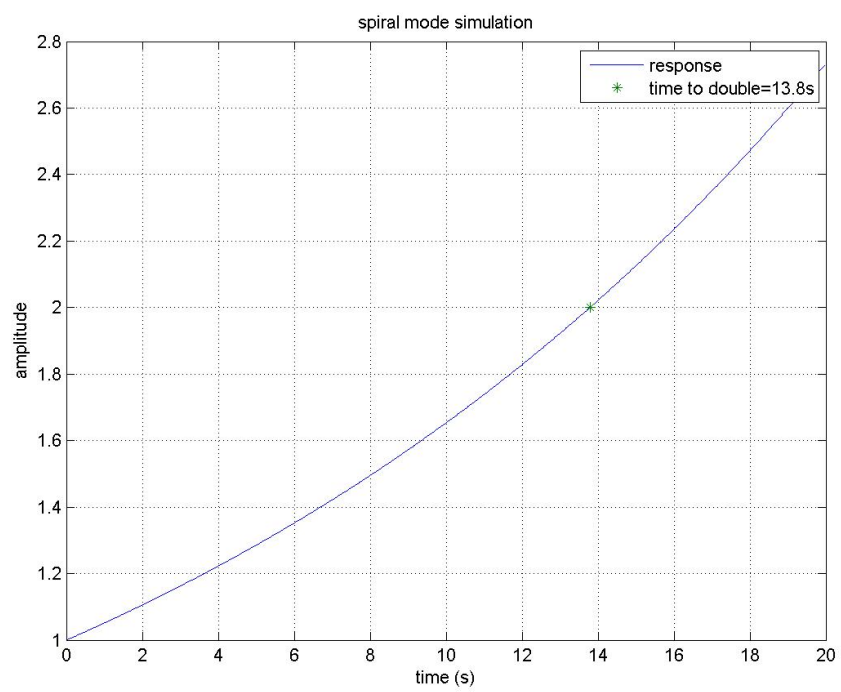
Figure 21: Time Simulation of Spiral Mode Subject to Unit Perturbation

8. Overall Design

The overall engineering drawings of our design can be seen in Appendix B. This figure also shows the loading possibility as well as the stability parameters. Wing design is summarized in Sec 5.6, tail design is summarized in Sec 6, and we have chosen a $9'' \times 6''$ propeller.

8.1. Mass Breakdown

Preliminary mass breakdown is shown in table 7.

Item	Mass(g)	% Mass
Motor & Propeller	90	6%
Battery & Receiver	110	7%
Fuselage & Landing Gear	60	4%
Cargo	570	39%
Wing	150	10%
Empennage	40	3%
Interconnects	50	3%
Margin	400	27%
Total Take-Off Weight (Proposed)	**1470**	**100%**

Table 7: Mass Breakdown

The majority of our mass is dedicated towards the cargo. In contrast, we have gone into great length to reduce weight on Fuselage by coming up with optimum cargo space allocation in consideration of aerodynamics as well as flight score. We have contributed a significant 27% of margin. The detailed components such as motor, propeller, battery, and receiver are allocated relatively insignificant amount because we have a better grasp on what they will weight. In fact we know the exact weighting for the component themselves. Our empennage estimate include the horizontal stabilizer, and any control surface and mechanisms, as well as the fin and rudder which we have not yet decided. Interconnects include the boom that connects empennage to our fuselage. Additional leeway in mass will go into making the boom more aerodynamic, or house more cargo as detailed design and analysis becomes available. We have tried to balance our cargo around the center of CG, and through a variable optimization script, we iterated the position of all the component with the estimated mass budget for an estimated CG. The final result is presented in a drawing in figure 22 of Appendix A.

Appendix A. Additional Stability Figures
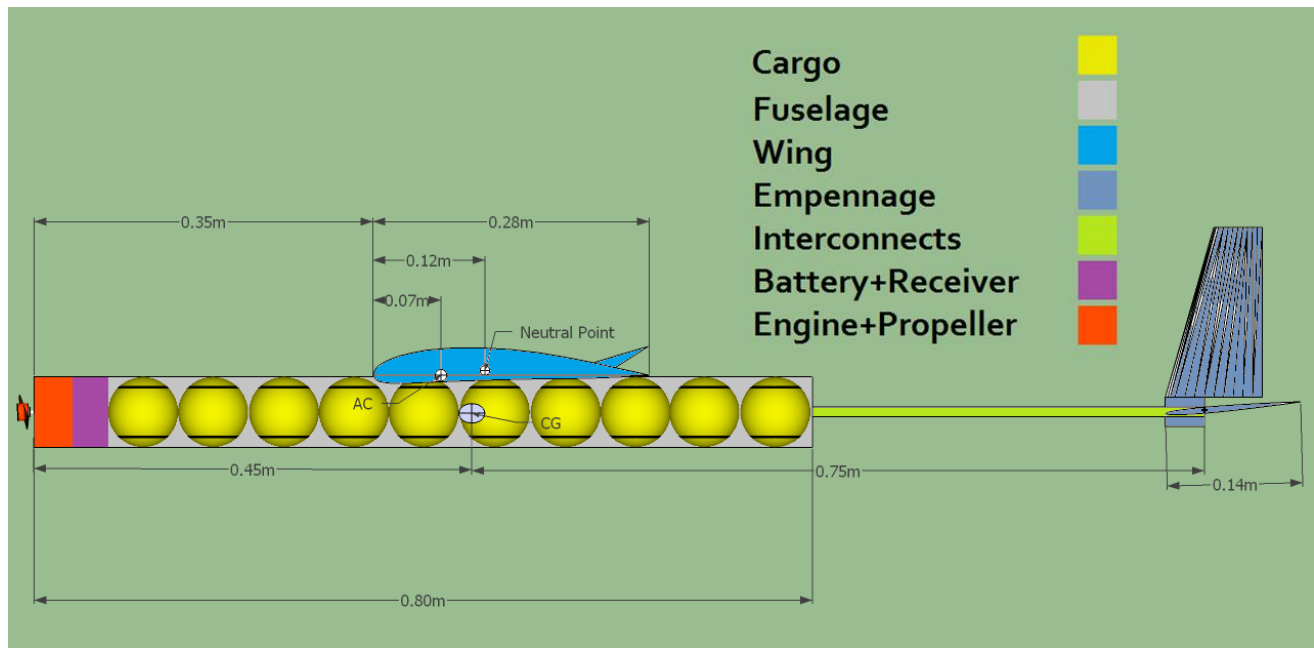
Figure 22: Proposed Weight Distribution and Stability Parameters
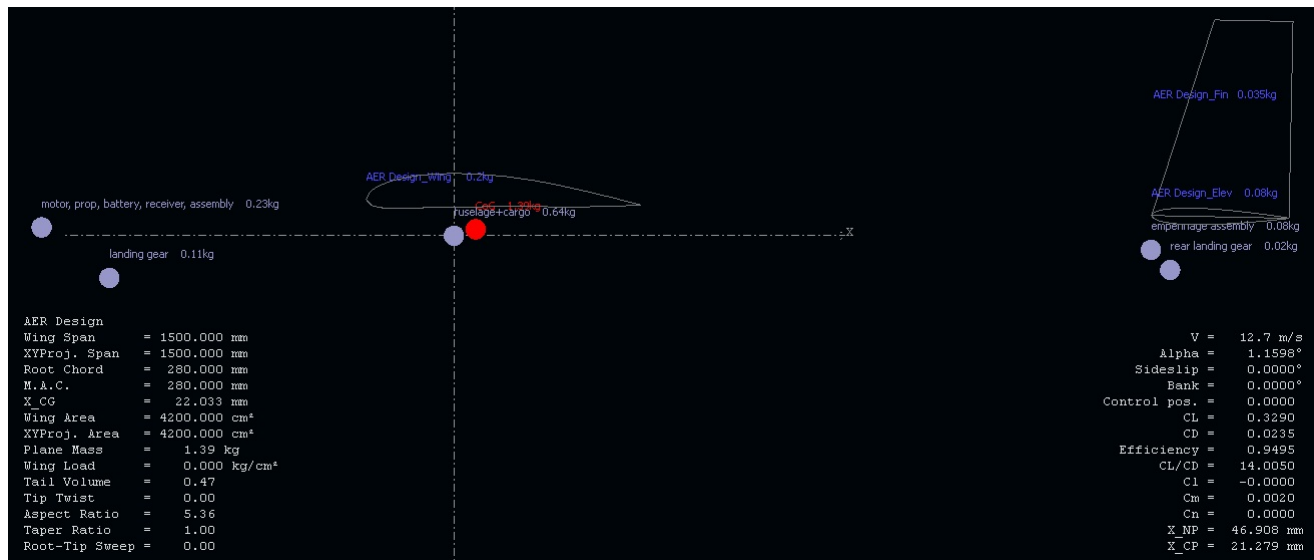
Figure 23: Detailed Mass Position and Stability Parameters

The origin is referenced at 450mm from the front tip of the plane, which is the original proposed CG. Design is done based around this point and iterated to give the values shown here. neutral point is at 46.908mm after origin and CG is located 22.033mm after origin. The plane mass is estimated at around 1.39kg at this point of time.

Appendix B. Engineering Drawings
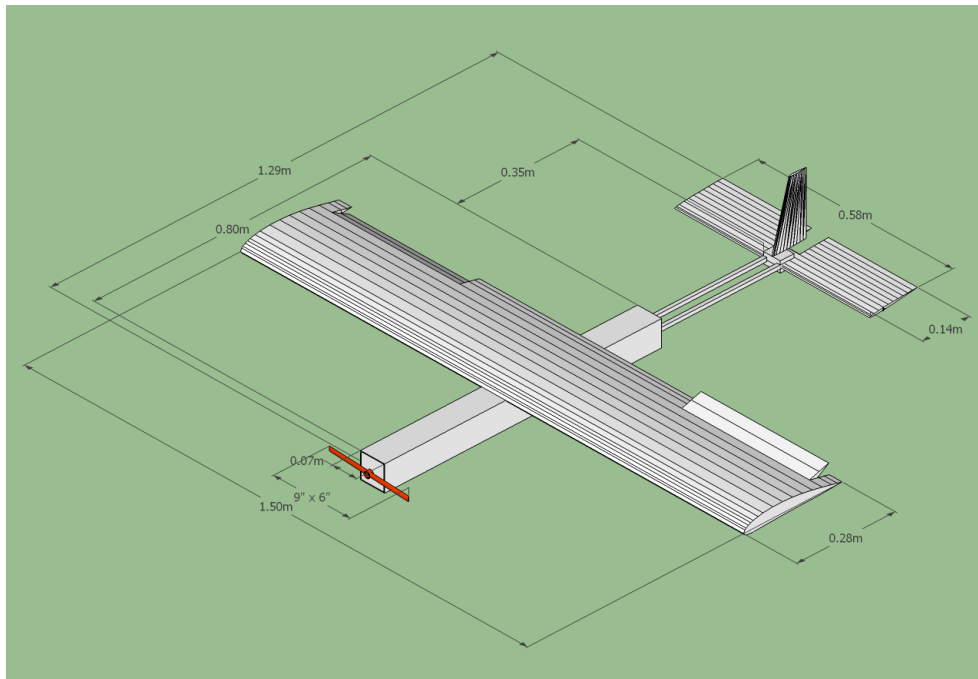
Figure 24: Plane Design 3D View
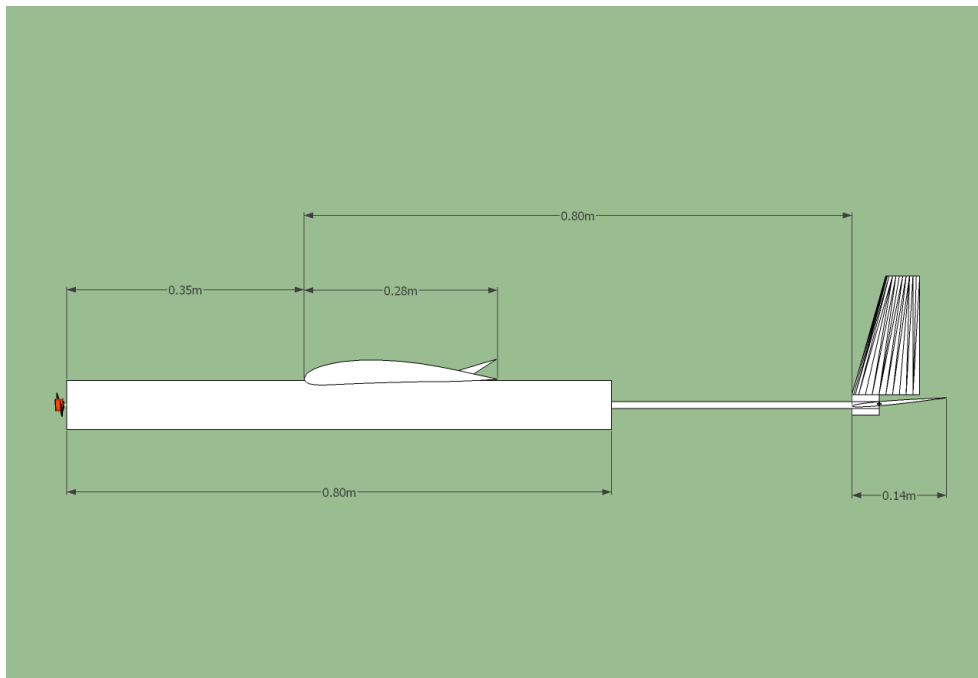
Figure 25: Plane Design Side View
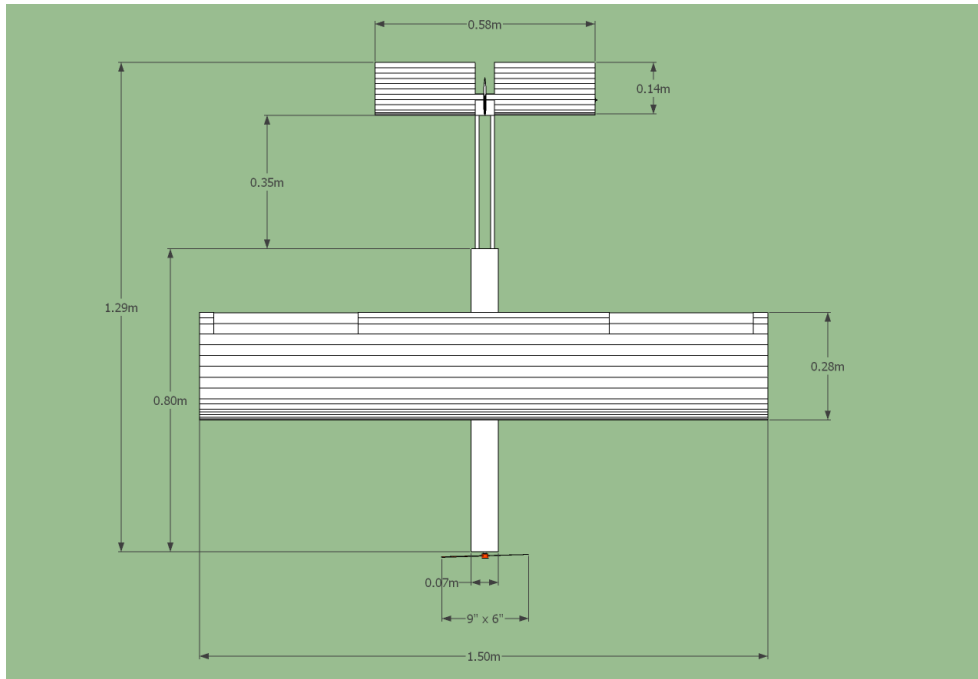
Figure 26: Plane Design Birds-Eye View

Appendix C. Airfoil Investigated
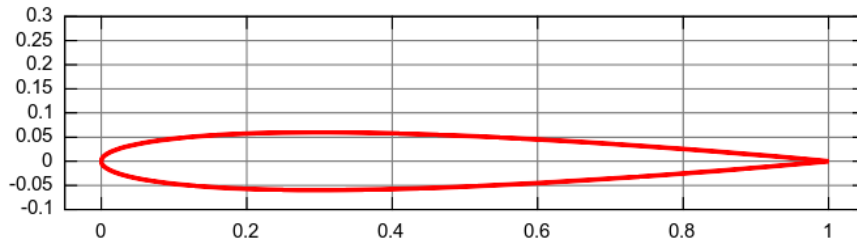
Figure 27: NACA0012 Airfoil Shape

$MaxC_L$	0.972
$Stall\,angle$	7.5
$Lower\,flatness$	17.1%

Table 8: NACA0012 Airfoil Information
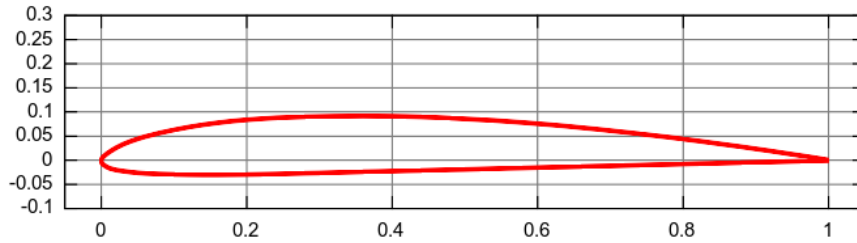
Figure 28: CLARK Y Airfoil Shape

$MaxC_L$	1.295
$Stall angle$	8.5
$Lower flatness$	71.8%

Table 9: CLARK Y Airfoil Information
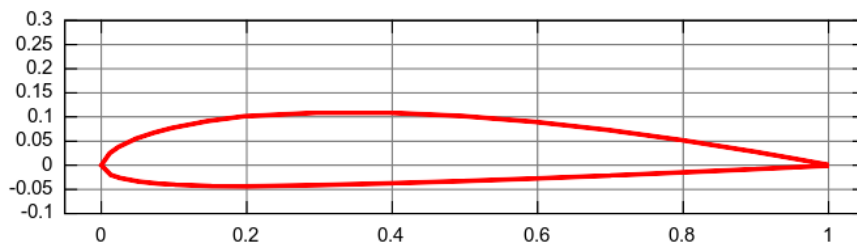
Figure 29: CLARK YM-15 Airfoil Shape

$MaxC_L$	1.598
$Stall angle$	14.0
$Lower flatness$	77.4%

Table 10: CLARK YM-15 Airfoil Information
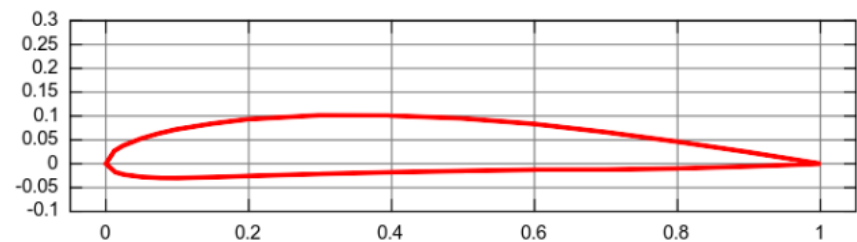
Figure 30: GOE526 Airfoil Shape